SELF-PROPAGATING HIGH-TEMPERATURE SYNTHESIS (SHS) OF ADVANCED HIGH TEMPERATURE MATERIALS

S. K. Mishra and L. C. Pathak

National Metallurgical Laboratory, Jamshedpur 831 007, India

ABSTRACT

Over the last few years, our research group at National Metallurgical Laboratory, Jamshedpur had contributed significantly on the fabrication of various advanced high temperature materials monolithic and composites namely ZrB_2, TiC, ZrB_2-Al_2O_3 and Al_2O_3-SiC by self-propagating high-temperature synthesis (SHS) technique. In this paper, the SHS processes developed at National Metallurgical Laboratory, Jamshedpur are reviewed. Ultra fine ZrB_2, TiC, TiC-Ni powder were prepared. New in-situ composites in the ZrB_2-Al_2O_3, Al_2O_3-SiC_w, TiC-Ni were prepared by the SHS techniques. The studies were focused on the SHS processing, mechanism of phase formation, microstructure evaluation, sintering of SHS produced powder and their property evaluation. A new combustion synthesis technique using a rapid heating self-propagating high temperature synthesis (RH-SHS) was made for the fabrication of in-situ Al_2O_3-SiC_w composite. Process for the in-situ preparation of 96% dense ZrB_2-Al_2O_3 by the SHS was developed.

Key Words : Self-propagating temperature, Synthesis, Diborides, Sintering, In-situ composite.

INTRODUCTION

The SHS is a well-known method for the fabrication of several high temperature ceramics, intermetallic and nano-composite materials in a single-step of processing. The SHS technique has inherent advantages over the other methods that require high temperature furnaces and longer processing times. Materials produced by the SHS method have advantages such as high purity of product, low energy requirements and relative simplicity of the process. The exothermic heat generated during SHS reaction is used for the completion of chemical reaction and once the SHS reaction is initiated at a particular ignition temperature (T_i), the combustion front propagated within the reactants at a particular combustion velocity to yield the final product. The major source of energy in a combustion synthesis technique is supplied from the exothermic heat of reaction. The feasibility of synthesising a given compound or composite through this route and sustainability of the wave front propagation mainly depends on the extent of heat liberated by the exothermic reaction(s) and the heat dissipated from the system to the surrounding [1]. The important parameter in this regard is the adiabatic temperature (T_{ad}), which is the maximum possible rise in temperature of the system due to the exothermic heat of reaction when the system is adiabatic. Empirically, it is known that a value of T_{ad} above 1800 K is essential for the self-sustainability of the combustion process [2, 3]. The adiabatic temperature, T_{ad} can be calculated by assuming complete conversion of the reactants to

the products. Since most of the exothermic reactions are initiated at a temperature (T_i) above the room temperature and for the calculation of the adiabatic temperature, the total enthalpy generated by the exothermic reaction is assumed to be consumed in increasing the temperatures of the products, and their is no heat loss to the surroundings. The total change of enthalpy, ΔHT_i at any temperature Ti can be given by

$$\Delta H_T = \int_{T_i}^{T_{ad}} \sum_i \Delta C_{P_i} dT \tag{1}$$

where, ΔH_T is the enthalpy change associated with the exothermic reaction, DCpi represent the difference between the specific heats of product i. and reactants at constant pressure. For simplicity, various phase transformations of the reactants and products are not considered in equation 1. The adiabatic temperatures for the different chemical reactions adopted by our group are presented in Table -1.

Table 1: Adiabatic temperature for different chemical reactions

Ti + C = TiC	(T_{ad} = 3200 K)
$ZrO_2 + B_2O_3 + 5Mg = ZrB_2 + 5MgO$	(T_{ad} = 2100K)
$3ZrO_2 + 10Al + 3B_2O_3 = 3ZrB_2 + 5Al_2O_3$	(T_{ad} = 2200K)
$3SiO_2 + 3C + 4Al = 2Al_2O_3 + 3SiC$	(T_{ad} = 2375K)

It is well known that various high temperature materials could be prepared by the SHS techniques. Amongst the various high temperature materials, the zirconium diboride, ZrB_2 is emerging as a potential advanced ceramic material because of its excellent properties- high melting point, hardness, elastic modulus and electrical conductivity, excellent chemical resistance to HCl, HF and other non-ferrous metals, cryolite and non-basic slags. The salient features of ZrB_2 are given in Table-2.

Table 2 : Properties of zirconium diboride

Density (g/cm³):	6.09
Lattice parameter (Å):	a=3.168,c =1.114
Crystal structure:	Hexagonal
Modulus of elasticity:	440-460 GPa
Hardness:	12-22 GPa
Melting point:	3313(K)
Electrical resistivity:	9.2(x10⁻⁶W cm)
Thermal conductivity:	23-25 (W/mK)

These excellent properties make ZrB_2 a potential material for use at high temperatures requiring wear, high temperature oxidation and corrosion resistance. Zirconium diboride has several applications, like cathodes for electrochemical processing of aluminium (Hall-Heroult process), evaporation boats, and crucibles for handling molten metals, thermowells, and thermocouple sleeves for high temperature use, wear parts, nozzles, armour, cutting tools and as dispersoid in metal and ceramic matrix composites to improve mechanical properties. Several techniques are established to prepare zirconium diboride powders. The different techniques are: from elements by melting, sintering or hot pressing, borothermic reduction of metal-oxides and boric oxide, reduction of the metal oxide with carbon or boron carbide, aluminothermic, magnetiothermic and silicothermic reduction of metal oxide- boric oxide mixture and self propagating high temperature synthesis (SHS) synthesis from elemental powder of boron and zirconium.

In the SHS of zirconium diboride [4], zirconium and boron metal powders are mixed together and ignited from the top. The ignition source is switched off as the surface reaches the required ignition temperature and the combustion wave propagates throughout the sample. The velocity of the combustion wave has been calculated to be as high as 25 cm/sec. Even though the SHS process has advantages, the use of elemental powder makes the process expensive. Hence, it is observed that in all the above processes, the time requirement is more and they require high temperatures in the range of 2000 to 2200°C to achieve 95% and above pure products or pure elemental powders are required as starting raw material making the process costly. The sintering of zirconium diboride is also known to be difficult due to its high melting temperature and covalent nature. Most often zirconium diboride powder is sintered at 2000-2200°C by hot pressing and pressureless sintering studies are very limited.

Though some reports on sintering of titanium diboride are available, very few reports are available in literature on the sintering of zirconium diboride powder [5]. Various binders such as Fe, Cr [6], CrB_2, Cu, Ni, NiB was used to get dense titanium diboride compacts. Owing to the high cooling rates and high defect concentrations, non-equilibrium metastable structures was expected to exist in the SHS produced powders, resulting in more reactive and enhanced sinterablity of the powders.

Besides the diborides, the other important high temperature materials include the carbides such as TiC, WC, SiC and in-situ composites. Recently, the alumina based ceramic matrix composites had shown promise as advanced materials for high temperature application because of their excellent refractoriness, low susceptibility to oxidation and good mechanical properties at elevated temperatures. Besides the conventional powder metallurgical route, synthesis of these composites by in-situ fabrication methods were gaining momentum because of certain inherent advantages. To indicate a few, in-situ fabrication mode eliminated the danger of handling carcinogenic compounds such as SiC whisker (SiC_w) which was one of the most widely used reinforcing material. Further, the chances of segregation in this route were relatively low compared to the mechanical mixing methods. The number of processing steps was also less in the in-situ fabrication technique than the conventional methods. So far several techniques for the synthesis of in-situ composites were reported. Some of the important in-situ composites were ZrB_2-Al_2O_3 and Al_2O_3-SiC.

The alumina (Al_2O_3) - zirconium diboride (ZrB_2) composite is an important technical ceramics for different technological applications [7, 8]. Such composite could

be used at high temperatures requiring wear, oxidation and corrosion resistance. The addition of zirconium diboride to alumina expected to have a better strength like titanium diboride- alumina composite. Titanium diboride dispersion in alumina had shown properties with higher strength, hardness and fracture toughness. The microstructure had shown no damage under very high impacts. Very few reports were available on zirconium diboride - alumina composite, in which they had prepared the composite powder by taking particulates of alumina and zirconium diboride. To the best of our knowledge, in-situ fabrication of zirconium diboride-alumina composites was not reported in literature. Aluminothermic reduction in a resistive heating furnace was used. These composites were found to enhance the mechanical strength and also alumina matrix was found to become conductive at 20vol% addition of zirconium diboride. The ZrB_2 addition was also advantageous over titanium diboride because it did not have many stable phases like titanium diboride. This made the composite favourable over TiB_2, however ZrB_2 had higher density than titanium diboride. Similarly, the SiC reinforced alumina composites are important for various structural applications that are exposed at high temperatures. Recently, the in-situ fabrications of Al_2O_3-SiC composites are also getting momentum.

In this paper, the different processes developed by our group for the fabrication of ZrB_2, TiC and in-situ composites such as, ZrB_2-Al_2O_3, Al_2O_3-SiC etc. are reviewed. The SiC reinforced alumina composites were fabricated by a new combustion synthesis technique named as the rapid heating self- propagating high temperature synthesis (RH-SHS) [9,10]. The effect of heating rates on various aspects of the SHS process will be discussed.

PREPARATION OF TiC AND TiC-Ni COMPOSITE POWDER BY SHS:

For the synthesis of TiC powder by the SHS route, stoichiometric amount of Ti (100-150µm) and amorphous carbon (<1µm) powder of commercial grade were taken as per the reaction mentioned in Table-1 and then mixed by a ball mill. The mixture was compacted by applying a load of 0.28GPa and subsequently ignited by an electrical Arc. Once the combustion initiated, the arcing was switched off. The schematic of the experimental set up is given in figure 1. Different amount (0-16.5 wt%) of Ni powder (~100mm) was also added with the reaction mixture and the SHS was carried out.

Graphite Electrode

Gas

Graphite Crucible

Sample S.S.

Gas
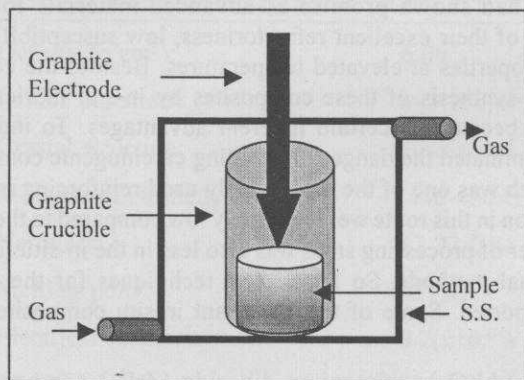
Fig. 1: Schematic of the SHS reactor

The SHS of TiC and TiC-Ni powder was described elsewhere [11]. The synthesized powder showed the formation of TiC and Ni phases (as the case may be) in the XRD patterns. The SEM of the synthesized powder showed the generation of fine TiC powders (Fig. 2). The SHS produced powder was compacted and sintered at various temperatures in inert atmosphere (Ar). The densities of the samples were measured by Archimedes principle of liquid immersion technique with an accuracy of ± 2%. The commercially available TiC powders are normally sintered above 2000°C for yielding good sintered products and often they are hot presses or hipped. The SHS produced powder could achieve to a maximum of ~ 92% densification when TiC -10Ni powder was sintered at 1800°C. The enhanced sintering of was possibly due to liquid phase sintering and high concentration of lattice defects and non-equilibrium structures present in the synthesized powders, which was resulted from the high rate of heating and cooling during combustion wave propagation.

Typical SEM image of the sintered pellets showing the densed microstructure are presented in figure 3. During sintering formation of Ni$_3$Ti intermetallic and its precipitation (needle type) in the matrix could be observed. The detailed sintering studies are published by Mishra (Pathak) et al. [12].
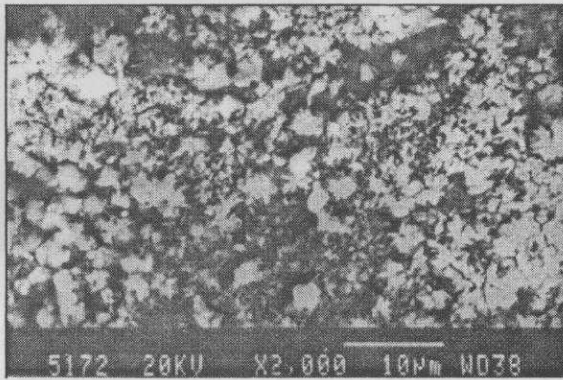
Fig. 2 : SEM image of the TiC powder
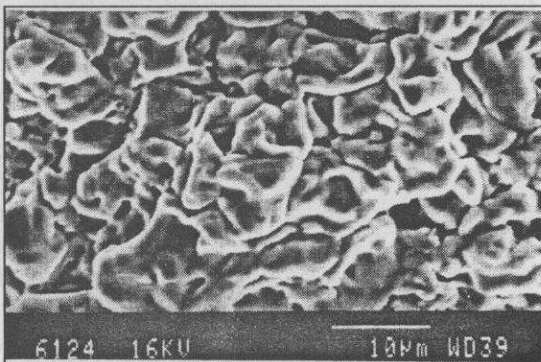
Fig. 3 : SEM image of TiC-10Ni pellet sintered at 1800°C for 1h

SHS preparation of ZrB_2 powder

For the synthesis of zirconium diboride (ZrB_2) powder by the SHS process, stoichiometric amount of zirconia or compound of zirconium (99% purity, particle size < 5 µm), India), boron oxide or compound of boron (99% purity, particle size < 40 µm) India) and Mg (99% purity, particle size <100 µm) India) was taken and mixed by a planetary ball mill (PM400 - Retsch, Germany) for 30 min at 300 rpm. The mixture was ignited from the top by an electrical arc in argon atmosphere as discussed earlier and schematically shown in figure 1. The reaction was carried out in a closed chamber flushed and filled with IOLAR-1 argon. After the completion of SHS reaction, the reacted product consisting of ZrB_2 and MgO, Mg was leached out. The reaction by-product, MgO was removed by dissolving in dilute HCl and washing with distilled water. No milling was required to yield the fine ZrB_2 powder. The XRD analyses of the final products showed only the presence of ZrB_2 in the leached powder. The presence of Mg and its compounds could not be detected in the XRD pattern and also by the EDX and ICP analysis. The detailed process was described elsewhere [13]. The SEM of the synthesized powder revealed the formation of sub-micrometer sized particles (Fig. 4) and the TEM showed the generation of ~ 100 nm powders (Fig. 5).
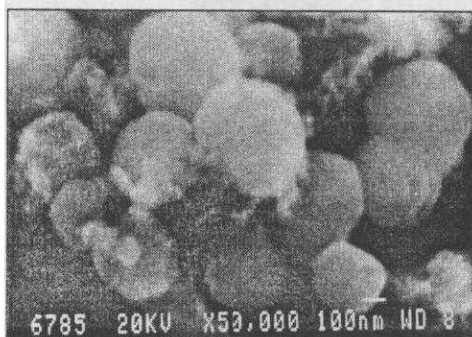
Fig 4 : SEM image of the ZrB_2 powders   Fig. 5 : TEM image of ZrB_2 powder
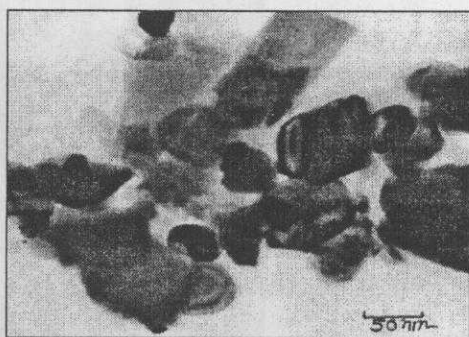
Similar to TiC, the zirconium diborides were also started sintering at low temperatures as low as ~1500°C and a maximum densification of 92% of the theoretical density could be achieved at 1800°C for 1h. During sintering, formation of zirconium oxide to the surface was detected. The microstructures showed faceted growth at few places, which indicated the evaporation condensation mechanism during sintering. The evaporation condensation mechanism in the boride systems is well known. However, the densification above 90% indicated the mass tranfer through volume diffusion process. The variation of density with the sintering temperature is plotted in figure 6. The excellent sinterability was primarily due to high surface energy of the ultra fine powder produced by the SHS technique and the high defect concentrations in the synthesised powders [14]. During sintering, except the formation of ZrO_2 at the surface no phase change could be detected in the sintered samples.

The SEM image of pellet sintered at 1800°C for 1h revealed the formation of dense packed structure with grain size ~ 20 mm (Fig. 7). In some of the samples melting due to formation of other low melting borides could be observed. From the sintering

equation [15], where the rate of densification at temperature T are expressed as:

$$\frac{d\rho}{dt} = \frac{K}{T} e^{-\frac{\Delta E}{kT}} \qquad (2)$$

yielded the value of activation energy, $\Delta E = 247.7 \pm 4$ kJ/mole. (K was the constant and k is the Boltzman constant). This activation energy possibly represented the mass transfer process of volume diffusion through grain boundary. For achieving more than 90% densification volume diffusion processes are required. The detailed of the sintering process were also published in literature [13]. The sintered pellets were having high electrical conductivity and had good mechanical properties. Extensive studies on the TEM of these sintered samples were investigated to find out the grain-boundary structures and the details are reported elsewhere [16].
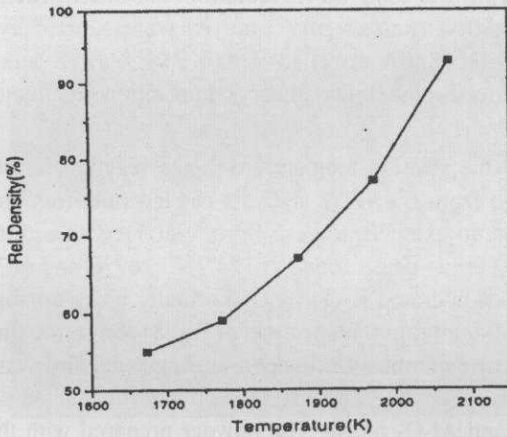
Fig. 6 : Variation of apparent density of ZrB_2 pellets with sintering temperatures
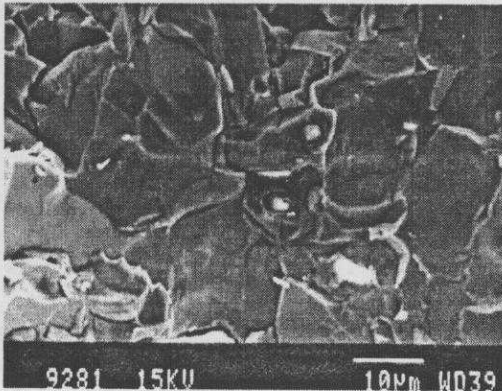
Fig. 7 : SEM image of ZrB_2 pellet sintered at 1800°C for 1h

SHS OF IN-SITU ZrB_2 -Al_2O_3 COMPOSITES:

The raw materials, zirconium oxide (99 % pure), fine aluminium (99% pure, < 5 μm in size) powder and boron oxide (99 % < 200 μm) powders, were mixed together in a ball mill. The mixture was compacted in the form of 20 mm diameter and 40-60 mm long cylindrical pellets. The SHS was carried out under argon atmosphere (0.5 MPa) in a closed reaction chamber. The pellets were ignited with an electrically heated tungsten coil placed on the top surface of the green pellets. Once the ignition of pellet started, the ignition source was switched off. A thermocouple (W-Re 5/20, 100 mm thick) was inserted from the bottom of the sample to 5 mm from the bottom end to measure the combustion temperature and the combustion velocity. The reactions were carried out for different amount of aluminium content (near the stoichiometric regime (28-32 wt%)) in the mixture. The phase analyses of the synthesised composites were carried out from the X-ray diffraction patterns of the crushed powder using Cu K_α radiation. The microstructural characterisation and elemental composition analysis of Zr and Al were studied by scanning electron microscope (SEM) JEOL 840A attached with KEVEX EDX analyser. The ignition temperature of the reaction for the stoichiometric composition was studied by the differential thermal analysis (DTA).

Experimentally the ignition temperature of the reaction for stoichiometric green mixture was measured from the DTA analysis carried out from room temperature to 1275°C, which showed an exothermic peak starting at 1168°C with the peak position at 1238°C. Several endothermic peaks found at 124.7°C, 167°C and 663°C due to moisture removal, dehydration of hydrated B_2O_3 (B_2O_3 normally picks up some moisture during storing) and melting of aluminium, respectively (Fig. 8). From the time-temperature plot obtained during SHS, the combustion temperature and velocity was measured to be ~ 2327K and ~5cm/sec respectively. The XRD patterns of the reacted powder showed only the presence of ZrB_2 and Al_2O_3 phase. The powder prepared with the lower aluminium content than the stoichiometric requirement, expectedly showed the presence of a very small amount of ZrO_2 phase. The unreacted B_2O_3 could not be detected due to its amorphous nature.

The powders prepared with high Al content did not show the presence of unreacted Al possibly due to oxidation by the presence of oxygen impurity in the IOLAR argon or due to low quantity of Al, which could not be detected by the XRD techniques. Microstructural investigation of the fracture surface showed insignificant variation with the Al content (28-32wt%) in the samples. The SEM showed the presence of two types of phases in the synthesised product, the large grains (10-20 mm) of Al_2O_3 and the small grains (0.5 to 3mm) of ZrB_2 (Fig. 9). At some places melt growth of Al_2O_3 was observed (Fig. 10) possibly due to attainment of high combustion temperatures at the reaction interface or due to precipitation of alumina and subsequent fusion by absorbing heat of reaction during SHS reaction between solid ZrO_2, liquid Al and liquid B_2O_3. Similar observations were also made during SHS of TiC-Al_2O_3 in-situ composites by Feng et al. [17]. The details of the ZrB_2-Al_2O_3 composite fabrication process were also reported elsewhere [18]. Further studies on the in-situ composites and sintering of these composites are being carried out and will be published in journals.
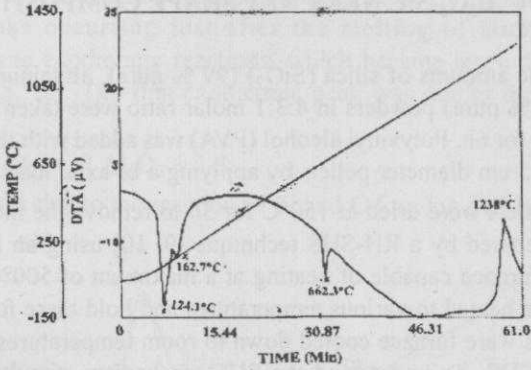
Fig. 8 : TG/DTA plot for $ZrO_2+B_2O_3+Al$ mixture in argon heated at the rate of $10^oC/min$
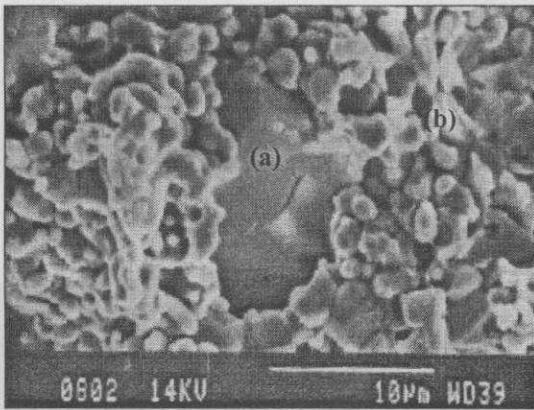
Fig. 9 : SEM image of ZrB_2-Al_2O_3 composite showing the particles of
(a) Al_2O_3 and (b) ZrB_2
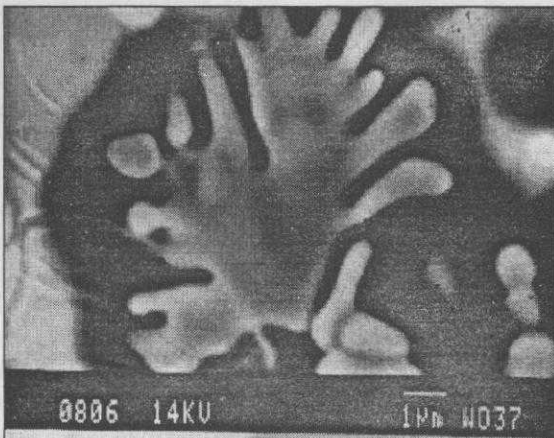
Fig. 10 : SEM image of ZrB_2-Al_2O_3 composite showing the melt type of growth

115

PREPARATION OF Al_2O_3-SiC NEAR NET SHAPE COMPOSITES BY RH-SHS TECHNIQUE

Stoichiometric amounts of silica (SiO_2) (99 % pure), aluminum (99 % pure) and carbon (graphite, 98% pure) powders in 4:3:1 molar ratio were taken in a stainless steel container and milled for 6h. Polyvinyl alcohol (PVA) was added with the powder mixtures and compacted to 2.5 cm diameter pellets by applying a bi-axial load of »100 MPa..

The green pellets were dried at 150°C for 3h to remove the moisture. The in-situ composites were prepared by a RH-SHS technique [9, 10] using an indigenously made graphite resistance furnace capable of heating at a maximum of 500°C per minute (Fig. 11). The pellets were heated to various temperatures and hold there for different periods and then the samples were furnace cooled down to room temperatures and characterized by the XRD, SEM/EDS. To understand the SHS mechanism, simultaneous differential thermal analyses (DTA) and thermo-gravimetric analyses (TGA) of the pellets were carried out in a SEIKO TG/DTA apparatus (Model No. 320) with varying heating rates. The reaction initiation temperature (Ti) was measured from the DTA plots using three-point method. Fractured surfaces of the samples were studied by a JEOL - 840A SEM system equipped with a KEVEX - EDS system. XRD analyses were carried out using $Cu-K_\alpha$ or $Co-K_\alpha$ radiations.

GAS OUTLET
TEMP. MONITORING PORT
GAS INLET
INSULATED TOP COVER
ELECTRICAL CONNECTOR
WATER COOLED M.S. CELL
GRAPHITE INSULATION TUBE
GRAPHITE HEATING ELEMENT
CARBON INSULATION POWDER
SAMPLE STAND
WATER INLET
WATER OUTLET
WATER COOLED BASE PLATE
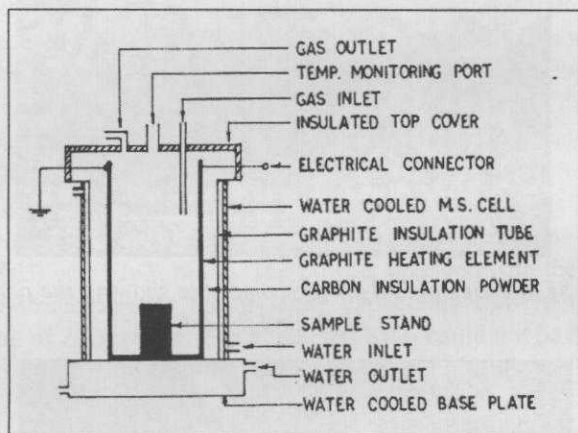
Fig. 11 : Schematic of the rapid heating graphite resistance furnace

In the RHS-SHS process, the very high rapid heating schedules were adopted to avoid the segregation of liquid aluminium and use the exothermic heat of the combustion reaction to achieve simultaneous densification in the synthesized composites. In this process, as the samples were heated rapidly to the sintering temperatures a sharp thermal gradient across the samples started the SHS reaction at one portion of the samples when it attained the reaction initiation temperature, Ti. At low heating rate i.e. 5°C per minute, the reaction initiation temperature was observed to be 723°C, which matched well with the reported value of 715 - 720°C in the literature [19]. Besides the endothermic peaks at 572°C and 660°C in the DTA thermograms, the exothermic peaks were observed after the melting of Al. The increase of reaction initiation temperatures (T_i) and peak

temperatures (T_p) with the heating rates indicated that the process was diffusion controlled. The exothermic peaks occurring just after the melting of aluminum were the superimposition of three exothermic reactions, which became more distinguishable at high heating rates (Fig. 12). The first exothermic peak was due to the aluminothermic reduction of silica i.e.,

$$4\ Al + 3\ SiO_2 = 2\ Al_2O_3 + 3\ Si \tag{3}$$
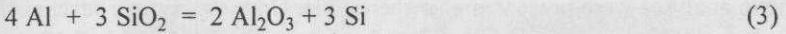
and the second peak was due to the reaction of Si and C forming SiC i.e.,

$$Si + C = SiC \tag{4}.$$
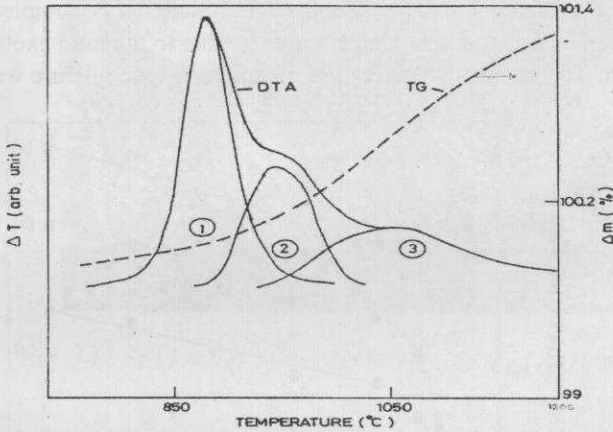
Fig. 12 : TG/DT plot of the Al+SiO₂+C powder mixture heated at the rate of 100°C/min

The third exothermic peak due to the oxidation of Al, Si or SiC by the traces oxygen present in argon gas was confirmed by the weight gain of the samples. The variation of the second exothermic peak temperatures, $T_{p(SiC)}$ for the SiC formation as a function of heating rates also showed a continuous increase of $T_{p(SiC)}$ with the heating rates and the lowest peak temperature for SiC formation was noted to be 867°C. The formation of SiC well below the reported value of the ignition temperature (1425°C) was possibly due to the localized attainment of high temperatures.

From the variation of peak temperatures, the apparent activation energy for the aluminothermic reduction process was calculated to be 240 ± 5kJ/mol from the Kissinger's plot. The excellent matching of the estimated apparent activation energy with the interdiffusion activation energy of Si and oxygen (241.7 kJ/mol) suggested that the reduction of silica by liquid aluminum in the present investigation was possibly controlled by the diffusion of oxygen through Si formed at the reaction interface. The Kissinger's plot for the estimation of activation energy for the process of silicon carbide formation showed a value of 255±7.5 kJ/mole, which was much higher than the reported inter-diffusion activation energy of Si and C (12.98 kJ/mole) and much lower than the self-diffusion of carbon in polycrystalline β-SiC (841±13.5 kJ/mole for lattice diffusion and 563 ± 8.7 kJ/mole for grain boundary diffusion) and also much lower than the activation energies for the self-diffusion of Si in β-SiC (912 ± 4.8 kJ/mole). The deviation of activation energies indicated that neither the diffusion of Si nor C through solid SiC was the rate-

controlling factor in the SHS of Al_2O_3-SiC composites. The activation energy of 240±5 kJ/mole for the first exothermic peak was close to the second activation energy indicating that the process of silicon carbide formation was possibly controlled by the liberation of Si in the aluminothermic reduction process. However, the contribution of chemical reaction between Si and C in controlling the overall reaction could not be ruled out. The details of the kinetic analyses were presented elsewhere [20]. Once the sample reaches the T_i, the SHS set in and the propagation of the flame front was completed within 7-10 seconds and we observed that the combustion reactions proceeded in two distinct stages. The first stage was associated with a considerable temperature rise due to highly exothermic oxidation reaction of aluminum. The second stage initiated after completion of the first stage and was marked by moderate temperature rise due to the mild exothermic reaction of SiC formation. The adiabatic temperature of stoichiometric mixture was calculated to be ~ 2375 K.
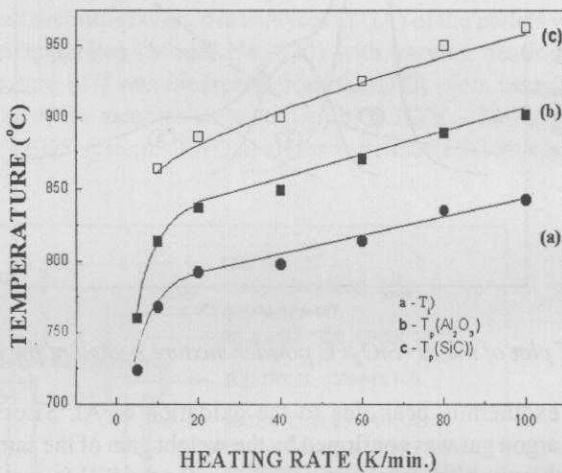
Fig. 13 : Variation of T_i, T_p and T_{pSiC} with heating rates

The presence of metallic Si in the samples was evident from the XRD patterns of the samples, which were not soaked at high temperatures for long periods confirmed the aluminothermic reduction of SiO_2. Some amounts of unreacted SiO_2 and metallic aluminium were also detected in those samples. A systematic study on the soaking time revealed that a soaking for ≈ 10 min was sufficient for the complete reduction of silica and a soaking period of ≈ 30 min was required for the completion of SHS reactions [10]. From the SEM studies the formation of SiC whisker was observed to be dependent upon holding temperatures, soaking temperatures and the rate of heating. We observed that the SiC whisker formation was prominent when the samples were rapidly heated above the melting point of Si i.e. ~ 1420°C. At 100°C per minute heating rate only formation of particulate was observed in most of the samples (Fig. 14) and where the heat dissipation was sluggish only in those areas SiC whisker was formed.The scanning electron microscopic image of the sample heated at 400°C/min from room temperature to 1450°C and soaked for 10 minutes showed the formation of SiC whisker throughout the sample and the quantity of whisker was also found to be more (Fig. 15). The formation of whisker

by liquid phase mass transfer process was evident in the RH-SHS process [20]. The amount and size of the whisker was also observed to increase with the processing temperature and time as evident from the SEM investigations.
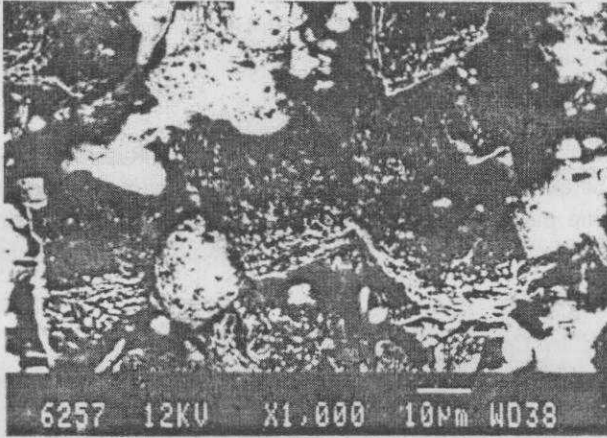
Fig. 14 : SEM image of the Al+SiO₂+C heated at 100°C/min

The photograph of the fabricated composite pellets shown in figure 16, indicated that the shape of the pellets remained unaltered after the RH-SHS. During SHS no distortion in the pellets could be detected this indicated that the RH-SHS could be used for the near net shape fabrication of Al_2O_3-SiC composites. This also confirmed the aluminothermic reduction of SiO_2 because a large volume of gas evolution during carbothermic reduction would result in deformed, porous powders product.
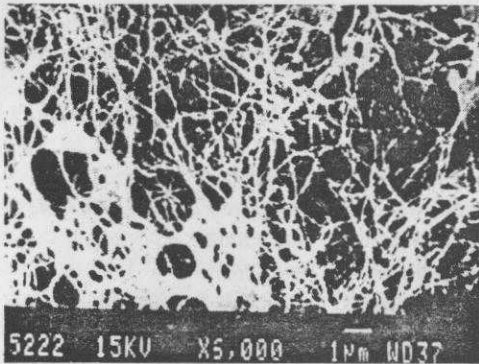
Fig. 15: SEM image of the Al+SiO₂+C heated at 100°C/min
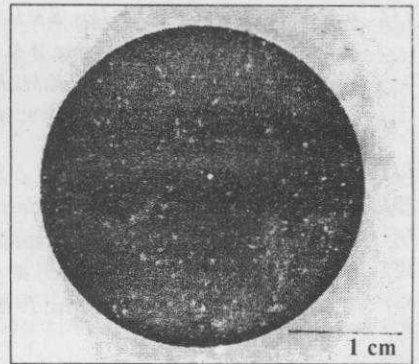
Fig. 16: Photograph of the composite pellet made by the RH-SHS technique

119

CONCLUSIONS

A number of SHS processes developed by our research group for the fabrication of various high temperature materials are discussed. Single-phase TiC, ZrB_2 and in-situ TiC-Ni, ZrB_2-Al_2O_3 composite powders were prepared by the SHS process. The SHS powders were also sintered to >90% densification. The RH-SHS process could be used for the near net shape fabrication of Al_2O_3-SiC in-situ composites. Several aspects of the SHS processes are emphasized.

ACKNOWLEDGEMENT

REFERENCES

[1]   Z. A. Munir, Am. Ceram. Soc. Bull. 67 (1988) 342.

[2]   N. P. Novikov, J. P. Borovinskaya and A. G. Merzhanov, In "Combustion processes in chemical technology and metallurgy" Ed. A.G.Merzhanov, 174 (1975), Chernogolovka.

[3]   C.R. Bowen and B.Derby, Br. Ceram. Trans. 96 (1997) 25.

[4]   Z. A. Munir, U. Anselmi-Tamburini, Mat. Sci. Rep., 3 (1989) 277.

[5]   J.Kecskes, T. Kottke. J. Am. Ceram.Soc. 73 (1990) 1274.

[6]   Duabdesselam, Z. A. Munir, J. Mater. Sci. 22, (1987) 1799.

[7]   S. P. Ray: Metall. Trans. A, 23A (1992) 2381.

[8]   S. Postrach, J. Potschke: J.Euro. Ceram. Soc., 20 (2000) 1459.

[9]   D. Bandyopadhyay, L. C. Pathak, S. K. Das, I. Mukhergee, R. G. Ganguly and P. Ramachandrarao, Mater. Res. Bull. 32 (1997) 75.

[10] D. Bandyopadhyay, L. C. Pathak, S. K. Das, Ravi Kumar and P. Ramachandrarao, Proc. International Conference on Recent Advances in Metallurgical Processes" Ed. Sastry et al.New Edge Publ. Delhi, India, (1997) 599.

[11] S. K. Mishra (Pathak), S. Das, R. P. Goel and P. Ramachandrarao, J. Mater. Sci. 16 (1997) 965.

[12] S. K. Mishra (Pathak), S. K. Das, A. Roy and P. Ramchandrarao, J. Mater. Res. 14 (1999) 3594.

[13] a. S. K. Mishra (Pathak), S.Das, S.K.Das and P. Ramachandrarao, J. Mater. Res.15 (2000) 2499.

      b. S.K. Mishra (Pathak), S.K. Das, A.K. Ray and P. Ramchandrarao, J.Am.Cerm. Soc. Nov. (2002)

      c. P. Ramachandrarao and S.K.Mishra- Zirconium diboride synthesis and sintering- Refractories & Furnaces- New options and new values, 31-39, 2000. Published by Allied publishers.

[14] S.K.Mishra, S. Das, L.C.Pathak, J. Mater. Res., (under review).

[15] R. M. German, Metal Powder Industries Federation, Princeton, New Jercy, (1994) 145.

[16] S. K. Mishra, S. Das, P. Ramachandrarao, J. Mater. Res. Nov. (2002).

[17] H. J. Feng and J. J. Moore, Met. & Mater. Trans. B, 26 (1995) 265.

[18] S. K.Mishra (Pathak), S. K. Das, P. Ramachandrarao, D. Belov, S. S. Mamyan, Met. Mater. Trans. A (In press).

[19] R. A.Cutler, K. M. Rigtrup and A. V. Virkar, J. Am. Ceram Soc. 75 (1992) 36.

[20] L. C. Pathak, D.Bandyopadhyay, S. Srikanth, S. K. Das and P. Ramachandrarao, J. Am. Ceram. Soc. 84 (2002) 915.